# THE CONTRIBUTION OF ABSORPTION LINES TO THE OPACITY OF MATTER IN STELLAR INTERIORS

ALBERT ARKING AND JACKSON HERRING
Goddard Institute for Space Studies
National Aeronautics & Space Administration
New York 27, New York

The structure and evolution of stars depends very sensitively on the opacity of the matter throughout the star. For stars of the sun's mass and greater, the bulk of the material is at temperatures above a million degrees, and an accurate knowledge of opacities at these temperatures is important for calculating the time scales of various phases of stellar evolution.

The absorption of radiation in the interiors of stars is due to electronic transitions which are grouped into three categories: free-free, bound-free, and bound-bound transitions. At temperatures of a million degrees and higher the bound-free transitions of the heavy elements are the dominant contributors to the radiative opacity, although at much higher temperatures the elastic scattering by free electrons becomes increasingly important.

The effects of the bound-bound transitions have always been difficult to estimate. Integrated over the frequency spectrum, the bound-bound absorption cross-sections are comparable to the bound-free, but since they absorb only in very narrow portions of the spectrum, albeit very strongly, their *over-all* effect on the opacity is small. This is due to the manner in which the absorptive processes enter the calculation of the structure of stellar interiors: as an average transparency or, more precisely, a weighted average of the *inverse* of the absorption coefficient called the Rosseland mean opacity. An infinitely narrow absorption line has no effect on the transparency because the amount of radiation contained in a very narrow portion of the black body spectrum is negligible. On the other hand, a line sufficiently broadened (e.g. as a result of high temperature and pressure) will affect the opacity with the full weight of the bound-bound cross section. The effect of discrete transitions on the Rosseland mean opacity, therefore, depends very importantly



Reprinted from the *Publications of the Astronomical Society of the Pacific*
(Vol. 75, No. 444, June 1963)

on the widths and shapes of the lines, as well as on their strength.

This paper reports a calculation of the contribution of the lines to the opacity of stellar material at conditions typical of stellar interiors (temperatures of 1 to $20 \times 10^6$ °K and electron densities of $\sim 3 \times 10^{25}/\text{cm}^3$). Our results indicate that the total Rosseland mean opacity is increased by $\sim 10$ to 40 percent above the continuous opacity for the Keller and Meyerott Group X mixture of elements.[1] The mass fractions of this mixture are hydrogen (.485), helium (.485), and heavier elements (.03); of the heavier elements the most important, at the temperatures under consideration, are iron, potassium, and aluminum. Their mass fractions are shown in the second column of Table III.

The difficulty in calculating the effects of discrete transitions in the past has been the lack of an adequate theory of line broadening for stellar conditions. The statistical theory of Holtsmark could take account of the broadening by the slow-moving ions but could not adequately account for the broadening by the faster electrons. Early attempts at handling electrons by means of the impact approximation did not include electron-induced transitions among nearly degenerate states.

A theory has been developed recently by Kolb and Griem[2] and independently by Baranger[3] which treats the electron effects in the impact approximation. In this approximation a characteristic profile is associated with each energy level of the radiating ion due to the finite lifetime of the state of the ion as a result of electron collisions. The width of the profile is determined by the frequency of collisions.

The broadening due to both ions *and* electrons has been calculated by Griem, Kolb, and Shen.[4] The ions are treated in a quasi-static approximation, as in the Holtsmark theory, and the electron impacts are assumed to occur in the static field produced by the particular ion configuration at the time of impact.

The field distribution at the site of the radiating ion is obtained from a statistical determination of the possible ion configurations. For our calculations we used a modified form of the Holtsmark distribution, in which the repulsion due to the

charge of the radiating ion was taken into account. Ion-ion correlations were included only to the extent that for the repulsive potential between the radiating and perturbing ions we used a screened Coulomb potential in which both ions and electrons contribute to the screening. This field distribution agrees with the cluster expansion theory of Baranger and Mozer[5] carried out to first order.

In folding the ion field distribution with the electron impact profile we follow the method outlined by Griem,[6] in which three approximations are made:

1. The linear Stark effect is used for the level shift due to the ion field.

2. An approximate expression is used for the electron impact profile (viz. a dispersion profile) which agrees with the general expression on the wings.

3. The Stark broadening parameters and the dipole moment matrix elements are averaged over the angular momentum states, using asymptotic expressions for the ion field distribution.

The use of the linear Stark effect is valid when splitting of the angular momentum states is small compared with the Stark splitting. Thus, when the field strength is greater than a certain value, the linear Stark formula is applicable, whereas below this value of the field strength—that is, in the core of the line profile—the quadratic Stark formula is applicable.

As long as the number of bound electrons is not too high, the value of the field strength at which the linear Stark formula is applicable is small enough so that the important region of the line profile—the outer region—is adequately covered. The errors that may occur in the core of the line are not too important because of the saturation effect associated with the Rosseland mean.

For similar reasons, the second approximation—which correctly treats the wings of the lines at the expense of the core—does not seriously affect the results.

Averaging over the angular momentum states was done throughout our calculations. At the high temperatures that we consider, the bound electrons are few and the splitting of the

angular momentum states is therefore not large.

Such an approach is consistent with our use of hydrogen-like oscillator strengths and the use of perturbation theory to calculate the screening constants and occupation numbers.

At temperatures of the order of a million degrees and lower, it is extremely difficult to justify the averaging over subshells, which is associated with the hydrogen-like treatment of the problem. One must note, however, that it is generally the elements with fewer bound electrons that contribute to the line absorption. For example, the iron lines are important contributors from 10 to 20 million degrees, but below 10 million degrees the potassium and aluminum lines are the main contributors.

A typical profile obtained in this manner is shown in Figure 1 for the iron 1 → 3 transition. $N_e$ is the number of electrons per cubic centimeter; $\phi$ is the ionizing potential divided by $kT$; $\beta_e$ is the electron broadening parameter—it gives an indication of the relative importance of electron broadening to ion broadening, and in the absence of ion broadening it is the average half-

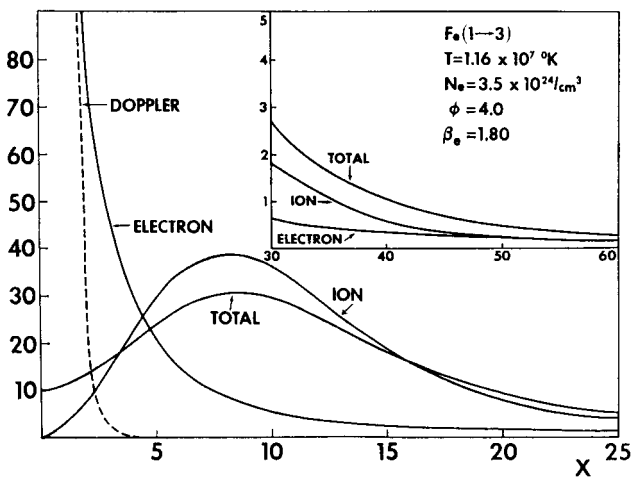


FIG. 1.—Profiles for the iron 1 → 3 transition are shown under the effects, separately, of electron impact broadening, ion broadening (Stark effect), and Doppler broadening. Both the electrons *and* ions contribute appreciably to the "total."

width of the line. The profiles are plotted as a function of $x = (\omega - \omega_0)/\omega_c$, where $\omega$ is $2\pi$ times the frequency, $\omega_0$ is the position of the center of the profile, and $\omega_c$ is a frequency unit depending upon the Debye length of the plasma and the transition involved.

The figure shows the effect of the electrons alone, and in our approximation it is simply a dispersion profile, with half-width $\beta_e$. The effect of ions alone is what one obtains from a modified Holtsmark statistical theory. The "total" is a folding of ion and electron effects. The Doppler broadening, which is not included in the "total," is shown to indicate that it is very narrow compared to electron-ion broadening.

The dependence of the electron width, $\beta_e$, on $\phi$ (the ionizing potential divided by $kT$) is shown in Table I for the important transitions at 5.8 million degrees. The percentages after each transition indicate the contribution (averaged over $\phi$) of these transitions to the entire bound-bound correction. Table I shows that the electron broadening is of increasing importance (relative to ion broadening) as $\phi$ increases, or as density decreases. Hence, the approximation of using a dispersion profile to represent the line shape is rather poor at high densities but is somewhat better at low densities.

The dependence of $\beta_e$ on temperature is shown in Table II. Again, the percentages indicate the contribution (averaged over $\phi$) of these transitions to the bound-bound effect. The depend-

TABLE I

VALUES OF THE ELECTRON BROADENING PARAMETER $\beta_e$

Mixture: Keller and Meyerott Group X ($X = .485$, $Y = .485$, $Z = .03$)

$T = 5.81 \times 10^6$ °K

| Transition | $\phi =$ 2 | 3 | 4 | 5 | 6 | 8 |
|---|---|---|---|---|---|---|
| K (1→2) 35% | 0.23 | 0.43 | 0.57 | 0.75 | 0.90 | 1.22 |
| K (1→3) 19% | 0.85 | 1.54 | 2.05 | 2.70 | 3.23 | 4.39 |
| K (1→4) 8% | 1.60 | 2.78 | 3.69 | 4.86 | 6.00 | 8.11 |
| Al (1→2) 8% | 0.16 | 0.76 | 1.00 | 1.18 | 1.36 | 1.81 |
| Al (1→3) 7% | 1.97 | 2.73 | 3.61 | 4.26 | 4.90 | 6.54 |
| Al (1→4) 3% | 3.71 | 4.93 | 6.52 | 7.68 | 9.09 | 12.08 |

TABLE II

VALUES OF THE ELECTRON BROADENING PARAMETER $\beta_e$

Group X Mixture ($X = .485$, $Y = .485$, $Z = .03$)

| Transition | $T =$ 23.2 × 10⁶ | 11.6 × 10⁶ | 5.8 × 10⁶ |
|---|---|---|---|
| Fe (1→2) | 1.1 (43%) | 0.8 (23%) | 0.4 (2%) |
| Fe (1→3) | 3.9 (30%) | 2.7 (11%) | 1.6 (<1%) |
| Fe (1→4) | 7.0 (12%) | 4.9 (4%) | 2.9 (<1%) |
| K (1→2) | 1.6 (6%) | 1.1 (29%) | 0.7 (35%) |
| K (1→3) | 5.9 (5%) | 4.0 (22%) | 2.5 (19%) |
| K (1→4) | 10.7 (3%) | 7.3 (10%) | 4.5 (8%) |
| Al (1→2) | | | 1.0 (8%) |
| Al (1→3) | | | 4.0 (7%) |
| Al (1→4) | | | 7.3 (3%) |

ence on temperature is seen not to be as striking as the dependence on $\phi$. The values of $\beta_e$ shown in Table II are also averaged over $\phi$.

In calculating the absorption of the discrete transitions, it is extremely important that one take into account the splitting of each transition into many lines because of the many possible electron configurations in which the radiating ion can be found. This configuration splitting of the lines contributes a factor of 2 or 3 in the effects of line absorption on the Rosseland mean.

We obtain the probability for the appearance of any configuration by treating the occupation number for each principle quantum number as an *a priori* probability that any electronic state associated with that principle quantum number is occupied. Each electronic state is treated independently with the result that electron-electron correlations are completely neglected. This approximation cannot be justified at low temperatures, where there are many bound electrons.

The continuous absorption coefficient on which our line corrections were based, as well as the electron occupation numbers used in the calculations, were obtained from an IBM 704 code developed at Los Alamos.[7] A few cases re-run using Strömgren's method[8] for computing the continuous absorption and occupation numbers indicate that the line corrections are not very sensitive to the methods used for obtaining these quantities.

## TABLE III

EFFECT OF LINES ON OPACITY
Group X Mixture ($X = .485$, $Y = .485$, $Z = .03$)

| | |
|---|---|
| Temperature | $5.81 \times 10^6$ °K |
| Density | 7.56 gm/cm³ |
| Electron Density | $3.37 \times 10^{24}$/cm³ |
| Ionizing Potential | 3.0 |

| $U$ | Mass Fraction | Transition | $K_\nu$ (cm²/gm) | $R$ | $\gamma$ |
|---|---|---|---|---|---|
| 15.59 | 0.00125 | Fe (1, 4) | 1.111 | 0.167 | 0.0003 |
| 14.97 | | Fe (1, 3) | 0.866 | 0.386 | 0.0011 |
| 13.03 | | Fe (1, 2) | 1.156 | 1.420 | 0.0049 |
| 8.43 | 0.00276 | K (1, 4) | 3.216 | 0.183 | 0.0132 |
| 8.04 | | K (1, 3) | 1.545 | 0.425 | 0.0495 |
| 6.89 | | K (1, 2) | 2.286 | 3.232 | 0.1224 |
| 3.91 | 0.00191 | Al (1, 4) | 10.77 | 0.042 | 0.0037 |
| 3.72 | | Al (1, 3) | 12.38 | 0.098 | 0.0078 |
| 3.17 | | Al (1, 2) | 14.48 | 0.413 | 0.0128 |
| 2.57 | | Fe (2, 4) | 26.50 | 0.063 | 0.0017 |
| | | | | Sum | 0.224 |

| | | |
|---|---|---|
| Opacity: | Continuous | = 4.943 cm²/gm |
| | Total | = 5.671 cm²/gm |
| | Line Contribution | = 0.15 |

In Table III we give a sample computation of the line opacity, broken down into contributions from various elements. The relevant physical conditions for the calculation are given at the top of the table. The mixture of elements is Keller and Meyerott's Group X mixture and its mass fractions for the important elements are listed in the second column. The other column headings are as follows: $U$ is the transition energy divided by $kT$; "Transition" gives the chemical symbol for the element contributing to the transition followed by the principle quantum numbers of the initial and final states; $K_\nu$ is the continuous absorption coefficient in cm²/gm at the listed transition energy; $R$ is the strength of the line relative to the continuum; and $\gamma$ is an estimate of the fractional contribution of the transition to the Rosseland mean opacity (ignoring the overlapping of lines). The last entries in the table give the continuous opacity

and the total opacity (with lines) in $cm^2/gm$ and their ratio.

One must bear in mind that each of these transitions is split into many lines because of the large variety of electronic configurations possible at these densities and temperatures. This configuration splitting is not shown. The effect of overlapping can be seen by comparing the sum of the individual $\gamma$'s with the final line contribution, "total" divided by "continuous" minus one. In Table III the reduction due to overlapping is seen to be the change from 22 percent to 15 percent.

It is to be noted from the percentage contribution of each line, which appears in parentheses in Table II for the Keller-Meyerott Group X mixture, that at the higher temperatures (above 10 million degrees) the line contribution comes primarily from iron and potassium. This is due primarily to the weighting function in the definition of the Rosseland mean.

A summary of the line corrections over a grid covering the interiors of stars of the order of the sun's mass and greater is given in Table IV for the Keller-Meyerott Group X mixture, containing 3 percent heavy elements. For stars of mass greater than 1.5 solar masses, the typical corrections are of the order of 15 percent or less for the interior regions, which are of importance in calculating the stellar structure.

Table V shows the line corrections when applied to the stellar mixture adopted by Arthur Cox. The corrections are

TABLE IV

CONTRIBUTION OF LINES TO OPACITY

Group X Mixture ($X = .485$, $Y = .485$, $Z = .03$)

| | Lines/Continuous for $T$ (°K × $10^6$) = | | | | |
|---|---|---|---|---|---|
| $\phi$ | 23.24 | 11.62 | 5.81 | 2.905 | 1.162 |
| 2 | 0.028 | 0.106 | 0.127 | — | — |
| 3 | .040 | .126 | .147 | — | — |
| 4 | .044 | .122 | .137 | — | — |
| 5 | .026 | .100 | .132 | 0.268 | 0.622 |
| 6 | .020 | .052 | .081 | .272 | .461 |
| 8 | .000 | .023 | .020 | .100 | .148 |
| 10 | — | — | .007 | .023 | .050 |

TABLE V

CONTRIBUTION OF LINES TO OPACITY
(Comparison with Los Alamos Results)

Mixture: Cox Solar Mix ($X = .744$, $Y = .236$, $Z = .02$)

| $\phi$ | Lines/Continuous for $T$ (°K $\times 10^6$) = 23.24 | 11.62 | 5.81 | 2.905 | 1.162 |
|---|---|---|---|---|---|
| 2 | .027 (.016) | .064 (.047) | .039 (.030) | — (.004) | — (.340) |
| 3 | .036 (.028) | .061 (.054) | .062 (.057) | — (.061) | — (.449) |
| 4 | .035 (.037) | .047 (.051) | .082 (.100) | — (.161) | — (.600) |
| 5 | .017 (.041) | .028 (.044) | .106 (.159) | .307 (.332) | .423 (.750) |
| 6 | .017 (.030) | .015 (.033) | .079 (.186) | .299 (.438) | .309 (.83) |
| 8 | .002 (0) | .006 (.007) | .020 (.067) | .101 (.238) | .100 (.62) |
| 10 | — (0) | — (.003) | .007 (.013) | .030 (.125) | .029 (.187) |

smaller primarily because of the lower mass fraction of heavy elements, only 2 percent.

The results of Cox and Stewart[9] are shown in parentheses in Table V. Although there is general agreement in the central portion of the table, the Los Alamos results are consistently higher than ours at lower densities, whereas our corrections are slightly higher at higher densities. The differences are due to the neglect of ion broadening in the Los Alamos calculations and to the broader profiles they used for electron broadening.

In comparing the electron impact broadening with the Stark broadening, we had observed in Table I that the electrons become more important as $\phi$ increases, that is, electron impact broadening tends to dominate at lower densities. Therefore, it is to be expected that at the lower densities their calculations would yield higher line-correction values, whereas the trend might go the other way at very high densities where the electron width becomes very small.

Several improvements in the program, which will permit extension of the calculations to lower temperatures, are presently under consideration. The treatment of ion broadening by the linear Stark effect and the electron broadening by degenerate electron widths will decrease in validity as the number of bound electrons increases.

The lines most affected by this approximation are those

associated with the $1 \rightarrow 2$ transitions. More accurate profiles which take proper account of the splitting between the 2S and 2P levels will result in better estimates of the line corrections at low temperatures, although it is unlikely that the present results, above a million degrees, will be affected.

The improved calculations will use the most up-to-date determination of stellar abundances. In calculating line corrections one must be careful to use the full set of elements. The grouping of elements with slightly different atomic numbers may have little or no effect on the continuous opacity, whereas it serves to coalesce lines that would otherwise be separate. The full mixture would therefore result in a larger line correction to the opacity than a reduced mixture in which elements were grouped.

A more detailed account of the present work, including the above improvements, will soon be published.

We wish to express our appreciation to Professor Bengt Strömgren for suggesting this problem and for his continual interest and advice.

---

[1] G. Keller and R. E. Meyerott, *Ap. J.*, **122**, 32, 1955.

[2] A. C. Kolb and H. R. Griem, *Phys. Rev.*, **111**, 514, 1958.

[3] M. Baranger, *Phys. Rev.*, **111**, 494, 1958.

[4] H. R. Griem, A. C. Kolb, and K. Y. Shen, *Phys. Rev.*, **116**, 4, 1959.

[5] M. Baranger and B. Mozer, *Phys Rev.*, **115**, 521, 1959.

[6] H. R. Griem, *Ap. J.*, **132**, 883, 1960.

[7] Los Alamos Code J-15, for the continuous opacity, was supplied to us by Arthur Cox.

[8] B. Strömgren, *Pub. Copenhagen Obs.*, **83**, 118, 1932; also, for example, S. Chandrasekhar, *Introduction to the Study of Stellar Structure* (Chicago: University of Chicago Press, 1939), chap. 7.

[9] A. Cox and J. Stewart, paper presented at 109th Meeting of the American Astronomical Society, Denver, Colorado, December 1961.